Testosterone-androgen receptor: The steroid link inhibiting TRPM8-mediated cold sensitivity

Dimitra Gkika, Stéphane Lolignier, Guillaume Grolez, Alexis Bavencoffe, Georges Shapovalov, Dmitri Gordienko, Artem Kondratskyi, Mathieu Meleine, Laetitia Prival, Eric Chapuy, et al.

Received: 4 September 2019 | Revised: 10 January 2020 | Accepted: 18 March 2020

DOI: 10.1096/fj.201902270R

RESEARCH ARTICLE

THE FASEB JOURNAL

Testosterone-androgen receptor: The steroid link inhibiting TRPM8-mediated cold sensitivity

Dimitra Gkika[1] | Stéphane Lolignier[2,3] | Guillaume P. Grolez[1] | Alexis Bavencoffe[1] | Georges Shapovalov[1] | Dmitri Gordienko[1] | Artem Kondratskyi[1,4] | Mathieu Meleine[2,3] | Laetitia Prival[2,3] | Eric Chapuy[2,3] | Monique Etienne[2,3] | Alain Eschalier[2,3] | Yaroslav Shuba[1,4] | Roman Skryma[1] | Jérôme Busserolles[2,3] | Natalia Prevarskaya[1]

[1]Univ. Lille, Inserm, U1003 - PHYCEL - Physiologie Cellulaire, Lille, France

[2]Université Clermont Auvergne, Inserm, Neuro-Dol, Clermont-Ferrand, France

[3]Institut Analgesia, Faculté de Médecine, Clermont-Ferrand, France

[4]Department of Neuromuscular Physiology, Bogomoletz Institute of Physiology NASU, Kyiv, Ukraine

Correspondence
Dimitra Gkika, Laboratoire de Physiologie Cellulaire, INSERM U1003, Bâtiment SN3, Département de Biologie, Faculté des Sciences et Technologies, Université de Lille, 59655 Villeneuve d'Ascq Cedex, France.
Email: dimitra.gkika@univ-lille.fr

Funding information
Institut National de la Santé et de la Recherche Médicale (Inserm); European Molecular Biology Organization (EMBO), Grant/Award Number: ALTF-161-2006; Institut Universitaire de France

Abstract

Recent studies have revealed gender differences in cold perception, and pointed to a possible direct action of testosterone (TST) on the cold-activated TRPM8 (Transient Receptor Potential Melastatin Member 8) channel. However, the mechanisms by which TST influences TRPM8-mediated sensory functions remain elusive. Here, we show that TST inhibits TRPM8-mediated mild-cold perception through the noncanonical engagement of the Androgen Receptor (AR). Castration of both male rats and mice increases sensitivity to mild cold, and this effect depends on the presence of intact TRPM8 and AR. TST in nanomolar concentrations suppresses whole-cell TRPM8-mediated currents and single-channel activity in native dorsal root ganglion (DRG) neurons and HEK293 cells co-expressing recombinant TRPM8 and AR, but not TRPM8 alone. AR cloned from rat DRGs shows no difference from standard AR. However, biochemical assays and confocal imaging reveal the presence of AR on the cell surface and its interaction with TRPM8 in response to TST, leading to an inhibition of channel activity.

KEYWORDS

hormone, ion channel, sensory neurons, thermosensation, transient receptor potential

Abbreviations: AR, androgen receptor; AR^{fl}, AR-floxed; AR^{wt}, wild-type littermates; DRG, dorsal root ganglion; I_{TRPM8}, TRPM8-mediated membrane current; NP_o, probability of TRPM8 opening; OX, orchidectomy; TRPM8, transient receptor potential melastatin member 8; TST, testosterone; HEK_{M8}, TRPM8-expressing HEK293 cells; $HEK_{M8/AR}$, HEK293 cells co-expressing TRPM8 and AR; PM, plasma membrane; PLA, proximity ligation assay; Ct, C-terminal tail; Nt, N-terminal tail.

Dimitra Gkika and Stéphane Lolignier shared first authorship.

Dimitra Gkika and Natalia Prevarskaya shared last authorship.

1 | INTRODUCTION

Sensing changes in environmental temperature is essential across species for the adaptation of organisms to their environment, and therefore, crucial to their survival. From this perspective, the identification of transient receptor potential (TRP) channels as highly sensitive molecular thermometers has substantially advanced our understanding of mammalian thermoreception at the cellular level.[1] The regulation of the activity of TRP channels is of primary importance for proper thermoreception and thermoregulation and accounts not only for pathological states, such as thermal dysesthesia, pain, or improper thermal homeostasis, but also plays a role in inter-individual variations in thermoreception. Indeed, multiple factors are known to influence thermosensitivity, including age, sex, body mass index, previous temperature experience and psychological state, as well as hormonal status.[2]

Regarding cold perception, TRPM8 is known to be one of the main cold receptors expressed in sensory neurons, and is directly activated by non-noxious cold (<28°C, with maximal activation around 18°C) or by chemicals evoking a cooling sensation such as menthol, icilin, or eucalyptol.[3] Using TRPM8-knockout mice, three independent groups have established that TRPM8 is indeed an important physiological detector of environmental cold.[4-6] In TRPM8-deficient mice, the ability to avoid cold temperatures is markedly suppressed, suggesting that TRPM8 activation is also involved in the generation of signals interpreted by the brain as being unpleasant.[4-6]

The TRPM8 modulators known so far are synthetic chemicals or active ingredients of plant extracts, with very few endogenous substances in the microenvironment of TRPM8-expressing cells being identified as channel regulators. In this respect, steroids have emerged as interesting candidates since they represent a large family of circulating mediators with important biological roles. Interestingly, epidemiological studies have indicated that among men lower testosterone (TST) concentrations may be associated with increased cold sensitivity,[7] while fluctuations in TST concentrations in a population of Norwegian men has been linked to variations in ambient temperature.[8] In addition, androgens are not only known to increase TRPM8 expression in prostate tissue [9,10] but TST has also recently been shown to rapidly modulate channel activity in vitro.[11-13] However, it is unclear how TST would act on thermoreception in vivo, and the exact molecular mechanism of the modulation of the sensation of cold by TST in sensory neurons remains elusive.[14]

The purpose of this study was, therefore, to determine how TST levels affect cold perception in vivo and to unravel the molecular mechanisms underlying this effect, by focusing on the TRPM8 channel as a putative link between the two. From this perspective, we took a multidisciplinary approach ranging from in vivo studies in rat and mouse models to single-channel electrophysiological measurements in primary sensory neurons, protein-protein interaction assays and confocal imaging in primary and overexpression cellular systems. The combination of these approaches allowed us to show that circulating androgens at a physiological level do indeed have an impact on the TRPM8-mediated perception of mild cold in both mice and rats. We observed that TST specifically inhibits TRPM8 activity in primary sensory neurons through its interaction with the cell-surface androgen receptor (AR).

2 | MATERIALS AND METHODS

2.1 | Behavioral animal studies

Experiments were performed on 150-200 g male Wistar rats (Janvier, France) 20-24 g male C57Bl/6J mice (Charles River, France) and *TRPM8*$^{-/-}$ mice (kind gift of Prof. D. Julius, UCSF, USA). We obtained floxed AR mice (stock no: EM:02579), whose generation has been previously described,[15] from EMMA. Transgenic *Nav1.8*-Cre mice were a kind gift from Prof. John N Wood (UCL, UK). Male mice expressing Cre recombinase under the control of the Nav1.8 gene promoter[16] were mated with floxed AR (B6N.129-Artm1Verh/Cnrm) female mice to generate ARfl Nav1.8-Cre and ARwt Nav1.8-Cre littermates. Detailed genotyping methods and primer sequences have been described previously.[16] Animals were acclimatized to housing conditions for at least 1 week prior to testing. They were housed in grouped cages in a temperature-controlled environment with food and water ad libitum. Behavioral experiments were performed blind to genotypes, in a quiet room, by the same experimenter for a given test taking great care to avoid or minimize discomfort of the animals.

For the siRNA assays Stealth RNAi were synthesized by Invitrogen. The sense sequences of siTRPM8 and the scramble control were 5′-CAGUGAUGUGGACAGUACCACAUAU-3′ and 5′-CAGGUAGGUACAAUGACCACUGUAU-3′, respectively. Intrathecal administrations of siRNA (10 μg/rat) were performed in a volume of 10 μl via direct transcutaneous injection (with a 25-gauge needle connected to a 25 μl Hamilton syringe) between the L5 and L6 dorsal spinous processes under anesthesia with isoflurane (3.5%). Treatments were randomized and all experiments were performed blind by the same experimenter using the method of equal blocks to avoid any uncontrollable environmental influence that might induce a modification in behavioral response. Treatments were randomized and all experiments were carried out according to the guidelines of the Committee for Research and Ethical Issues of IASP.[17]

In cold-avoidance test, two hot/cold plates (Bioseb, France) were placed side by side so that the adjacent thermal surface (each 16.5 × 16.5 cm) were enclosed in a single Plexiglas chamber (34 × 17×25 cm). The temperature of each plate could be controlled individually over the −3 to 65ºC range. Exploration of the plates by animals was recorded over 3 minutes by tallying the cumulative time spent on each plate. The temperature of one of the plates (reference) was maintained at a constant value of 25ºC, and the fraction of time spent on the second plate (test plate), which temperature varied between experiments, was calculated. The number of crossings was also recorded as a measure of general exploratory behavior.[18]

In the tail immersion test, the tail of the animal was immersed in a water bath (set at different temperatures ranging from 6 to 48°C) until withdrawal was observed (cut-off time 30 seconds).[19] Withdrawal latencies from three consecutive measurements were averaged out.

2.2 | Surgical procedures

All surgeries were performed on day 1 under anesthesia and strict sanitized conditions. Castrations were performed on day 1 via scrotal route by removing epididymal fat pads with the testes. The sham-castrated animals were opened, and their testes were dissected but not removed. Operated animals were then sutured, and the injured areas were disinfected with betadine solution and sprayed with aluspray (Vetoquinol).

To add the desired quantity of exogenous androgens for comparison with control animals, we implanted, at day 8, Silastic medical-grade silicone tubing (1 cm length, 2.5 cm length, or 3.5 cm length 0.078 ID × 0.125 OD; Dow Corning, Midland, MI) filled with TST (Sigma) subcutaneously over the scapula. As shown previously, these implanted silicone tubing filled with TST restore 50%, 100%, and 150% respectively of normal circulating TST.[20] One end of the tubing was sealed with adhesive (Silastic Medical Adhesive; Dow Corning). After loading with the hormone, the unsealed end was sealed with adhesive. After the adhesive had hardened, the implants were put overnight in distilled water. The implants were inserted on day 8 in pockets formed over the dorsal area of the scapula. The incised area was disinfected, and then, sutured.[20] The behavioral analyses were performed between days 14 and 21 after surgery.

2.3 | Cells and electrophysiology

Neurons were isolated from the lumbar dorsal root ganglion (DRG) of adult Wistar rats (250-300 g) using enzymatic digestion procedure described elsewhere.[21] Cell suspension was plated onto Petri dishes filled with 10% of fetal calf serum-and 8 μg/mL gentamicin-supplemented DMEM ("Gibco," UK) culture medium, and incubated for 18-24 hours at 37°C in the 95% air 5% CO_2 atmosphere, prior to using in electrophysiological experiments. For the whole-cell patch-clamp recordings, patch pipette was filled with Cs-based intracellular solution (in mM): 140 CsCl, 2 $CaCl_2$, 1 $MgCl_2$, 8 EGTA, 10 HEPES, pH 7.4, while bathing the cells in the standard extracellular solution (in mM): 140 NaCl, 5 KCl, 10 Glucose, 10 HEPES, 2 $CaCl_2$, 1 $MgCl_2$, pH 7.3.

HEK_{M8} cells were cultured as described previously[22] and TRPM8 expression was induced with tetracycline 24 hours before experiments. Western blot analysis have shown that TRPM8 protein expression in HEKM8 cells reaches maximum after 3 hours of tetracycline (2 μg/mL) induction, and then, remains steady for up to 48 hours.

Patch-clamp experiments were performed using Axopatch 200B amplifier and pClamp 10 software (Molecular Devices, Union City, CA) for data acquisition and analysis. Patch pipettes were fabricated from borosilicate glass capillaries (World Precision Instr., Inc, Sarasota, FL) on a horizontal puller (Sutter Instruments Co., Novato, CA) and had resistance of 2-3 MΩ for whole cell and 6-10 MΩ for single-channel recordings. Single-channel recordings were carried in cell-attached patches made to DRG neurons and $HEK_{M8/AR}$ cells. Cells were immersed in high-K+ solution (in mM: 150 KCl, 5 glucose, 10 HEPES, 1 $CaCl_2$, 2 $MgCl_2$, pH 7.3, adjusted with KOH) in order to keep membrane potential close to zero. Pipettes were filled with the same KCl solution, to keep recording conditions symmetrical.

Recorded activity was quantified by performing a single-channel search analysis using the pClamp 10 software. Stimulation of TRPM8 by both mild cold and application of 100 μM of menthol led to high levels of TRPM8 activity, with typical P_{open} in excess of 0.5. Therefore, simple rejection of traces that, at any point, exhibited multiple conductance levels provided a reliable way to select appropriate traces. Statistical analyses, *t*-tests, and Gaussian fits to amplitude distributions were carried out using the Microcal Origin software. Values are expressed as mean ± SEM, unless indicated otherwise.

2.4 | RT-PCR and quantitative real-time PCR analysis

DRG were homogenized with Precellys 24 using CK14 tubes containing ceramic beads (Bertin technologies, Ozyme, France) at 5000 rpm for two cycles of 20 seconds in Trizol Reagent (ThermoFisher Scientific, USA) and total RNA was isolated and reverse transcribed as described previously.[22] The AR coding sequence was then cloned in the pGEM-T Easy vector (Promega, France) using the following

primers pair 5′- ATGGAGGTGCAGTTAGGGCT-3′/5′-TCACTGTGTGTGGAAATAGATGGGC-3′. Custom made primers were purchased from (Eurogentec, Belgium) and long PCR was carried out with the High Fidelity Phusion DNA Polymerase (ThermoFisher Scientific, USA) and verified by sequence analysis.

TRPM8 expression levels were quantified by quantitative real-time PCR on a CFX96 Real-Time PCR Detection System. TRPM8 mRNA levels were quantified with the primer pair 5′-GGATCTTCCGCTCTGTCATC-3′/5′-TCATCTAGCTCCACGCACAG-3′. The housekeeping gene HPRT was used as an endogenous control to normalize variations in RNA extractions, the degree of RNA degradation, and variability in reverse transcription efficiency. Primers for HPRT were 5′-TAAGTTCTTTGCTGACCTGCTG-3′/5′-CCCGTTGACTGGTCATTACA-3′. To quantify the results, we used the comparative threshold cycle method described by Livak and Schmittgen.[23]

2.4.1 | Immunocytochemistry and confocal imaging

DRG neurons and $HEK_{M8/AR}$ were washed twice, fixed with 4% of formaldehyde-1X PBS for 15 minutes, washed three times, then, permeabilized in PBS-gelatin (Phosphate buffer saline, gelatin 1.2%) supplemented with 0.01% Tween 20 and 100 mM glycine for 30 minutes at 37°C. For the TST, surface labeling cells were treated with FITC-BSA-TST (Sigma) at room temperature for 1 min prior to fixation. Afterward, cells were incubated with primary antibodies: 1/100 goat polyclonal anti-TRPM8 antibody (Antibodies online), rabbit anti-AR (1/100 Santa Cruz) in PBS-gelatin at 37°C for 1.5 hours. After thorough washes, the slides were treated with the corresponding secondary antibodies: Rhodamine Red-X -labeled anti-goat (Jackson ImmunoResearch, dilution: 1/300), Alexa Fluor 488-labeled anti-rabbit (Jackson ImmunoResearch, dilution: 1/250) and Rhodamine Red-X -labeled anti-rabbit (Jackson ImmunoResearch, dilution: 1/250), diluted in PBS-gelatin for 1 hours at room temperature. The slides were then incubated with 0.3% Sudan Black) in 70% ethanol in order to reduce autofluorescence, washed twice, and mounted with Mowiol®. Fluorescence analysis was carried out using a Zeiss LSM 700 confocal microscope and Image J analysis software (NIH). For freshly isolated rat and mice DRG, confocal imaging was performed using LSM 510 META confocal workstation. FITC fluorescence was excited by 488 nm Argon laser and emitted light was captured at 505-530 nm. Rhodamine Red-X fluorescence was excited by 543 nm line HeNe laser and captured above 560 nm. DAPI fluorescence was excited by a 405 nm blue diode laser and the emitted light was captured at 470-500 nm. TRPM8 and AR antibodies were validated on freshly isolated DRGs from TRPM8 knockout and AR knockout mice as shown in Figure S3.

2.4.2 | Calcium imaging

Dorsal root ganglia neurons from ARwt Nav1.8-Cre and ARfl Nav1.8-Cre adult male mice were quickly collected in ice-cold Hanks' balanced salt solution (HBSS) and incubated 45 minutes at 37°C in 5% of CO_2 in a digestion enzyme mix containing: collagenase type III (5 mg/mL, Worthington), dispase (10 mg/mL, Gibco), glucose 10 mM, and HEPES 5 mM in Ca^{2+} and Mg^{2+}-free HBSS. DRGs were subsequently transferred in Dulbecco's modified Eagle's medium (DMEM) supplemented with heat-inactivated, charcoal-stripped Fetal Bovine Serum 10%, L-Glutamine 2 mM, Minimum Essential Vitamins solution 1× (Gibco), Penicillin/Streptomycin 100 UI/mL, Sodium Pyruvate 1 mM, and nonessential amino acids solution 1× (Gibco) and gently triturated using fire-polished glass Pasteur pipettes. After centrifugation, cells were suspended in supplemented DMEM and plated on poly-L-lysine and laminin-coated glass coverslips. Neurons were kept at 37°C in 5% CO_2 and used for calcium imaging experiments within 2 days after culture.

On the day of experiment, cells were washed twice in DMEM and incubated for 45 minutes at 37°C under gentle shaking in DMEM containing 4 μM Fura-2 AM (ThermoFisher) and 0.04% pluronic acid. Neurons were washed twice in a Krebs-Ringer solution containing: NaCl 140 mM, KCl 3 mM, $MgCl_2$ 1 mM, $CaCl_2$ 2 mM, D-glucose 10 mM, and HEPES 10 mM, pH 7.4, 300 mOsm. Fura-2 calcium binding was monitored by alternatively illuminating cells at 340 and 380 nm with an exposure time of 200 ms for each wavelength. Fluorescence emission at 510 nm was acquired every 2 seconds using an Ando Zyla sCMOS camera and recorded using the MetaFluor software (Molecular Devices). 340/380 nm fluorescence intensities ratios were normalized using ΔF/F0, where ΔF is the ratio subtracted by the ratio at the start of the experiment (F0).

During experiments, neurons were continuously superfused with 35°C Krebs-Ringer. Menthol and TST were dissolved in 96% of ethanol, which was used as vehicle when indicated. At the end of the experiment, excitable cells were identified by the application of high-KCl Krebs-Ringer solution (NaCl 93 mM, KCl 50 mM, $MgCl_2$ 1 mM, $CaCl_2$ 2 mM, D-Glucose 10 mM, and HEPES 10 mM, pH 7.4, 300 mOsm). Cells displaying an increase of at least 50% of their ΔF/F0 (calculated between the last acquisition before perfusion and the observed peak within the stimulation period) were included in the analysis. Among them, cells were considered as cold- or menthol-responsive for an increase of at least 40% of their ΔF/F0 upon stimulation.

2.4.3 | Biotinylation

Cells were subjected to cell surface biotinylation and precipitated after lysis with neutravidin-agarose beads (Pierce Rockford, IL, USA) as described previously in Gkika et al[24] For the immunoblot analysis, we used the anti-TRPM8 antibody (1/1500, Alomone Labs Ltd, Jerusalem, Israel) and rabbit anti-AR (1/400 Santa Cruz).

2.4.4 | Immunoprecipitation assay

HEK293 cells were transfected with CFP-tagged AR and His-tagged TRPM8. 48 hours after transfection, cells were washed twice with PBS and incubated on ice in lysis buffer (1% of Triton X-100, 1% sodium deoxycholate, 150 mM NaCl, 10 mM $NaKPO_4$, pH 7.2, and antiprotease cocktail; Sigma-Aldrich). After centrifugation (12 000 g for 10 minutes at 4°C) of the lysates, protein concentration was determined by BCA assay (Thermo Fischer Scientific). An equal amount of supernatants was incubated overnight at 4°C with 40μL His-tag beads (dynabeads His-tag, Thermo Fischer Scientific) in IP buffer (20 mM NaH_2PO_4, 150 mM NaCl, pH 8). The pellet was washed three times in IP buffer, resuspends in SDS sample buffer, heated at 95°C for 5 minutes, and separated on 10% of precast SDS-PAGE gels (Biorad). SDS-PAGE gels were analyzed by immunoblotting using rabbit anti-androgen receptor (AR) (1:400; Santa-Cruz, N-20) and rabbit anti-TRPM8 (1:400; Abcam, ab109308) antibodies. Each experiment was repeated at least in triplicate.

2.4.5 | GST-fusion proteins and pull-down assay

TRPM8 N- and C-terminal tail GST-fusion proteins were produced and purified as described previously.[24] For the direct interaction assay, PCMV-TNT AR, PCMV-TNT DBD/LBD, or PCMV-TNT NBD vectors were translated in vitro using the TNT Quick Coupled Transcription/Translation Systems kit (Promega) and the FluoroTect GreenLys in vitro Translation Labeling System (Promega) as per the manufacturer's instructions. In vitro translated proteins were incubated overnight at 4°C together with the purified GST-fusion proteins in presence or in absence of TST. Subsequently, beads were washed extensively and bound proteins were eluted with SDS-PAGE loading buffer, separated on 10% of SDS-PAGE gels and visualized by fluorescence imaging or immunoblotting using anti-AR (1:400; Santa-Cruz, N-20) and anti-GST (1:1000) antibodies (Bio-Imager Amersham Imager 600, GE, Healthcare, France). Each experiment was repeated at least in triplicate.

2.5 | Proximity ligation assay

Duolink® In situ red starter kit goat/rabbit (Sigma-Aldrich) was used according to the manufacturer's instructions. Cells transfected or not were seeded in confocal FluoroDish (World Precision Instruments) and were fixed after the TST treatment. After 10 minutes of fixation and permeabilization with 4% PFA cells were incubated in the blocking buffer (provided with the kit) for 30 minutes at 37°C in a humidified chamber. Cells were then incubated with the primary antibodies mentioned above diluted in the antibody diluents for 2 hours. For the rest of the protocol, the manufacturer's instructions were followed and images were acquired by confocal imaging (Zeiss LSM700) using z-stack superposition (Zen 2010 software, Zeiss). Appropriate controls were performed by incubating cells with both primary antibodies separately and gave no puncta.

2.6 | Drugs and chemicals

Testosterone, dihydrotestosterone, 17-β-estradiol, progesterone, menthol, were obtained from Sigma-Aldrich. Icilin was obtained from Tocris. Steroids were prepared as stock solutions at 10 μM in absolute ethanol, kept at −20°C, protected from light, and diluted into extracellular solution prior to experiments.

2.7 | Data analysis

Data are expressed as mean ± SEM Statistical significance was determined by two-way analysis of variance (ANOVA) followed by Bonferroni's multiple comparisons test or Tukey's method as indicated. Differences between two groups were analyzed by student *t*-test. The statistical analyses were performed using the Prism6 (GraphPad, USA) and Microcal Origin software.

3 | RESULTS

3.1 | Circulating TST reduces sensitivity to mild cold in rats

To check to what extent the level of circulating androgens impacts cold sensitivity in vivo, we conducted behavioral studies on male rats with different levels of circulating TST. In order to set androgen levels in these animals, we performed orchidectomy (OX) and infused with 50%, 100%, or 150% exogenous TST supplementation into their circulation. We first examined the cold sensitivity of OX male rats with strongly reduced circulating TST levels as compared to

sham-operated animals, using a standard thermal sensitivity test: measuring the rats' tail withdrawal latency in response to immersion in a water bath set at different temperatures, from noxious cold (6ºC) to noxious heat (48ºC). As shown in Figure 1A, lowering the androgen levels of male rats led to a clear reduction of their tail withdrawal latency in the range of cold temperatures: from 16 to 20ºC (Figure 1A), indicating that decreased TST level enhances sensitivity to mild cold. Consistent with this, the infusion of OX rats with exogenous TST via implanted mini-pumps restored the tail withdrawal latency up to control levels (Figure 1A). Notably, OX did not affect the animals' sensitivity to noxious cold

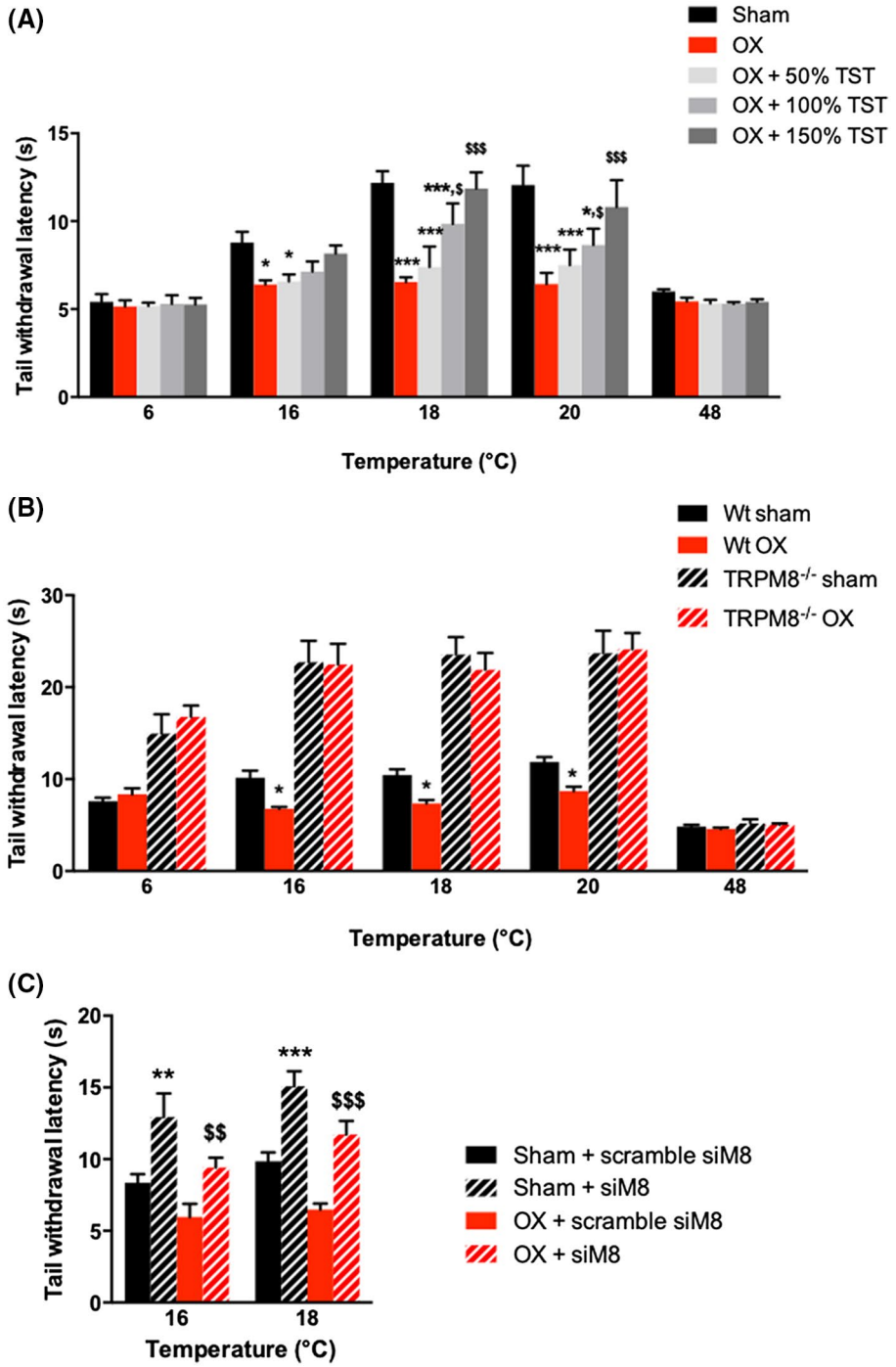

FIGURE 1 Testosterone levels tune TRPM8-mediated cold perception in rats and mice. Tail-withdrawal latencies at specified water bath temperatures in sham-operated (sham) or orchidectomized (OX) male rats A, as well as in sham-operated and OX wild-type (WT) and TRPM8$^{-/-}$ male mice. B,C, Comparison of tail withdrawal latencies at 16ºC and 18ºC in control (sham) and OX male rats treated with scrambled or TRPM8-targeting siRNA (siM8). Data are expressed as means ± SEM, statistical significance was determined by two-way ANOVA followed by Bonferroni's multiple comparisons test, n = 6-10 (*$P < .05$; **$P < .01$; ***$P < .001$ relative to sham and $^{\$}P < .05$; $^{\$\$}P < .01$, $^{\$\$\$}P < .001$ relative to OX)

(6°C) (Figure 1A), indicating the recruitment to the signaling pathway of the mild-cold-sensitive TRPM8 rather than the noxious-cold-sensitive TRPA1 channel.[25]

Similar results were also obtained with a second cold-avoidance behavioral test, in which OX male rats showed increased avoidance of a surface with a temperature ranging from 19 to 21ºC compared to controls. Again, this difference could be eliminated by the infusion of exogenous TST (Figure S1A). Thus, taken together, these experiments led us to believe that the level of circulating TST could strongly contribute to the tuning of mild-cold perception in the range of the TRPM8 cold sensitivity. Notably, quantitative PCR assays showed that OX per se and TST supplementation did not influence TRPM8 mRNA levels in the dorsal root ganglia (DRGs) of animals (Figure S1B), suggesting that in contrast to non neural cells, particularly prostate epithelial cells,[9,10] TRPM8 expression in the peripheral nervous system is not androgen-dependent.

3.2 | Circulating TST reduces cold sensitivity in both rats and mice through a TRPM8-dependant mechanism

To directly assess the involvement of TRPM8 in the TST-mediated regulation of cold sensitivity, we conducted the same behavioral tests on TRPM8-knockout animals generated through the targeted deletion of a genomic region encoding a part of the amino-terminal domain.[4] The aforementioned behavioral results showing the influence of TST on mild-cold sensitivity in rats were fully reproduced in wild-type but not in TRPM8$^{-/-}$ mice. Indeed, the tail immersion test showed that OX in wild-type mice led to the shortening of the tail withdrawal latency on average by 27% in the 16-20°C range (Figure 1B) while in TRPM8$^{-/-}$ mice the tail withdrawal latency not only increased dramatically, but OX failed to affect its duration (Figure 1B). Consistent with this, in the cold-avoidance test, wild-type OX mice spent on average 20% less time on 17-21ºC surfaces compared to their sham-operated counterparts, whereas in the case of TRPM8$^{-/-}$ mice, the time spent on 17-21ºC surfaces was found to be about 20% longer than that for wild-type controls, but there was no difference in latency between OX and control animals (Figure S2A).

In parallel, we utilized a siRNA-mediated knockdown strategy in male rats. The sequence targeted by TRPM8 siRNA (siM8) is located within the channel's pore region, resulting in the silencing of all putative functional TRPM8 isoforms. The protocol was based on previous studies demonstrating efficient silencing of ion channels in sensory neurons in vivo[26] and consisted of periodic (twice a day for 3 days) intrathecal injections of siRNA inbetween the L5 and L6 vertebrae of OX or sham-operated male rats. Quantitative RT-PCR showed that following knockdown, TRPM8 mRNA expression in the lumbar dorsal root ganglia (DRG) of sham-operated and OX male rats decreased by 43% ± 8% and 35% ± 6%, respectively (Figure S2B). In line with the results from knockout mice, the siRNA-mediated silencing of TRPM8 in sham-operated rats resulted in a longer latency to tail withdrawal at 16ºC and 18ºC (Figure 1C), consistent with a decrease in channel expression. In OX rats, the injection of anti-TRPM8 siRNA also led to a delay in tail withdrawal latency at 16ºC and 18ºC, similar to what we observed in knockout animals.

3.3 | TST inhibits native TRPM8-mediated currents in sensory neurons

Altogether the results obtained in the TRPM8-deficient rats and mice suggest that TST regulates mild-cold sensitivity in vivo via the activity of the cold receptor channel TRPM8 without affecting the channel expression. We, therefore, assessed the effect of TST on TRPM8 channels in DRG sensory neurons isolated from rats.

We first examined whether the TRPM8-mediated membrane current (I_{TRPM8}) in DRG neurons could be modulated by TST. In these experiments, we only used small-diameter DRG neurons, which in response to menthol (100 μM) developed I_{TRPM8} with characteristic biophysical properties (Figure 2A). The subsequent application of 10 nM TST caused the suppression of the current by 83% ± 12% (Figure 2A,B). To make sure that the observed I_{TRPM8} suppression was physiologically relevant, we conducted current-clamp studies. We found that the menthol-induced depolarization and associated action potentials (APs) were abolished by 10 nM TST (Figure 2C). Thus, physiological concentrations of TST are capable of suppressing the electrical firing induced in sensory neurons by the activation of the cold transducer TRPM8.

To investigate how the activity of TRPM8 was affected by TST at the single-channel level, we studied the currents in cell-attached mode in small DRG neurons. A subset of these patches exhibited currents characteristic of the TRPM8 channel, as evidenced by voltage and mild-cold sensitivity (the absence of response at 37°C and activation by mild cold (20°C) of single-channel currents of characteristic conductance), as well as sensitivity to menthol (100 μM), which was tested at the end of the data acquisition, following TST application[27] (Figure 2D-F). However, a majority of the patches from TRPM8-expressing DRG neurons exhibited multiple conductance levels, limiting our analysis to a characterization of the overall probability of TRPM8 opening (NP_o). Figure 2F shows that application of TST (10 nM) significantly inhibited the activity of native TRPM8 channels expressed in DRG neurons. The effect of TST is fast, within 20-30 sec upon application, which

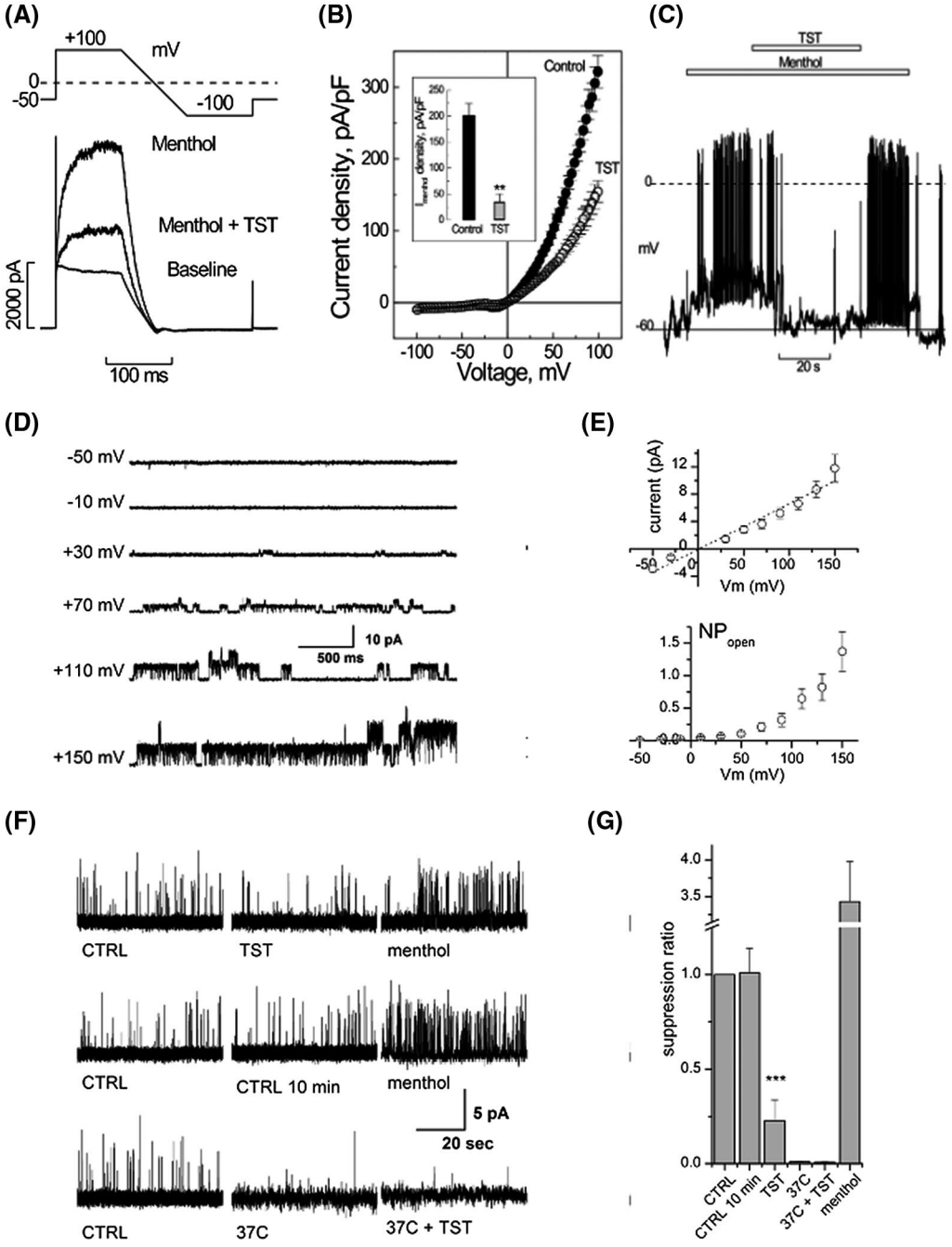

FIGURE 2 Testosterone inhibits the TRPM8 current in native DRG neurons. A, Representative recordings of the baseline current in DRG neurons at 32°C and currents after consecutive applications of menthol (100 μM) and menthol plus TST (100 nM); the voltage-clamp protocol is shown above the recordings. B, Averaged I-V relationships (mean ± SEM, statistical significance was determined by Student *t*-test, n = 5) of the current in the presence of menthol (100 μM, black symbols, control) and menthol plus TST (100 nM, open symbols); inset shows quantification of the effects of TST on the density of menthol-activated I_{TRPM8} at +100 mV. C, Suppression by TST (100 nM) of menthol-evoked action potential firing in DRG neurons; the recording of the membrane potential of neurons was performed in current-clamp mode; the application of menthol (100 μM) caused depolarization and AP firing, while the application of TST in addition to menthol caused hyperpolarization and cessation of AP firing. D, Representative TRPM8 activity in cell-attached patches on DRG neurons at indicated membrane potentials shows the characteristic voltage-dependence of the channe'sl activity. Summary curves of the IV relationship (upper) with the characteristic single-channel conductance of 67 ± 5 pS and voltage-dependent open probability NPopen (lower) are shown in (E). F, Representative TRPM8 activity in cell-attached patches on DRG neurons at an applied potential of 100 mV under basal conditions at mild cold temperature (20°C, CTRL) as well as 37°C and following application of testosterone (TST, 10 nM), and then, menthol (100 μM), to verify the identity of the recorded single ion channel. G, Quantification of TRPM8 NP_o suppression (relative to basal NP_o at 20°C) by TST (10 nM) in DRG neurons Data are expressed as means ± SEM, statistical significance was determined by pairwise Student *t* test against control, n = 6); ***$P < .001$

can be considered acute if we take into account diffusion of the added agent to the cells. Quantification of the TST effect showed a TRPM8 NP_o suppression of about 80% (Figure 2G). These results point to a direct nongenomic action of TST on TRPM8.

3.4 | TRPM8-mediated cold sensitivity involves the classic AR

To assess the mechanism of modulation of TRPM8-mediated cold sensitivity by TST, we initially tested the possible involvement of the classic AR in signal transduction. Although TRPM8 expression in the DRG is well established, little is known about AR expression in these neurons.[28] We successfully amplified the mRNA of the full-length AR using reverse transcription PCR (Figure 3A). Its cloning in a TA vector and subsequent sequencing confirmed that it was a classic non-mutated AR.

AR protein expression was then assessed using immunohistochemistry in DRGs freshly isolated from male rats. This revealed that AR was not only present in sensory neurons but colocalized with the TRPM8 channel at the cell periphery (Figure 3B). Interestingly, the colocalization of the two proteins was still observed following pretreatment with 10 nM TST, but not after pretreatment with 100 nM TST, which causes the translocation of AR to the nucleus (Figure 3B).

The presence of AR and its colocalization with the TRPM8 channel at physiological TST concentrations suggest the possible recruitment of AR in the inhibition of TRPM8-mediated cold sensitivity by androgens in vivo. To clarify the role of AR in this process, we used conditional AR knockout mice in which AR was knocked-out specifically in neurons positive for Nav1.8 (a marker of small nociceptive sensory neurons), obtained by crossing Nav1.8-Cre mice with AR-floxed (AR^{fl}) mice. We then subjected these animals to the tail immersion test, with temperatures ranging from noxious cold (6ºC) to noxious heat (48ºC), and found no difference in basal thermal sensitivity between AR^{fl} Nav1.8-Cre mice and their wild-type littermates (AR^{wt} Nav1.8-Cre). Consistent with our previous observations, the castration of these animals led to mild-cold hypersensitivity in AR^{wt} Nav1.8-Cre mice. Interestingly, AR^{fl} Nav1.8-Cre OX mice, which lack a functional AR, lost their hypersensitivity to mild cold (18°C, 20°C), similar to observations in WT OX animals (Figure 3C). We further tested whether TST affects calcium fluxes in DRG neurons of both AR^{wt} Nav1.8-Cre mice and AR^{fl} Nav1.8-Cre OX mice. Calcium imaging experiments showed that TST impairs the response to menthol and cold of AR^{wt} Nav1.8-Cre mice but not AR^{fl} Nav1.8-Cre OX mice (Figure S4) demonstrating thus that the AR is a necessary component for TST action on TRPM8-mediated cold sensitivity.

3.5 | TRPM8 activity inhibition via cell surface AR is specific to TST

To investigate whether the inhibition of TRPM8 channel activity is characteristic for TST, but no other related steroids, we used a cellular overexpression system: HEK293 cells co-expressing TRPM8 and AR. TRPM8 single-channel activity was recorded in cell-attached configuration at room temperature (ie, 20°C) in control cells, after a 10 min exposure to 10 nM TST or 17β-estradiol, and following menthol application. Our results (Figure 4A,B) clearly demonstrate a suppression of TRPM8 activity by TST but not by 17β-estradiol or progesterone, and the augmentation of channel activity following menthol application.

To study the TST effect on TRPM8 in more detail, we compared unitary TRPM8 activity of TRPM8-expressing HEK293 cells (HEK_{M8}) lacking AR with that in HEK293 cells co-expressing TRPM8 and AR ($HEK_{M8/AR}$), at gradually increasing TST concentrations, followed by application of 100 μM menthol to induce maximal activation of TRPM8. Figure 4C shows sample TRPM8 activity under these conditions and Figure 4D compares average activity levels in HEK_{M8} and $HEK_{M8/AR}$ cells in the presence of 10 pM, 1, 10, or 100 nM TST and 100 μM menthol, normalized to basal TRPM8 activity for each cell type. As can be seen, TST slightly potentiates TRPM8 activity in the absence of AR, in line with previously published results,[29] while it induces a dramatic suppression of TRPM8 activity in cells expressing AR at TST concentrations known to activate AR.

The above electrophysiological data clearly demonstrate the specific and rapid (and thus, likely nongenomic) effect of TST on TRPM8 activity. However, though the suppression of TRPM8 channel activity by TST evidently required the presence of AR, its binding to AR at the cell surface remained to be proven. To assess the possible surface binding of TST, we used a fluorescent plasma-membrane-impermeable form of TST, BSA-FITC-TST. HEK_{M8} and $HEK_{M8/AR}$ cells were incubated with BSA-FITC-TST and the fluorescent signal analyzed using confocal microscopy. Interestingly, only $HEK_{M8/AR}$ cells showed surface fluorescence due to BSA-FITC-TST (Figure 5A).

The localization of AR at the cell surface was further confirmed by biotinylation assays in $HEK_{M8/AR}$ cells. These experiments showed that AR was present in the plasma membrane (PM) fraction independently of the presence of TRPM8, even though TRPM8 expression increased AR concentration in the biotin fraction by 32.6% ± 3.7% (Figure 5B).

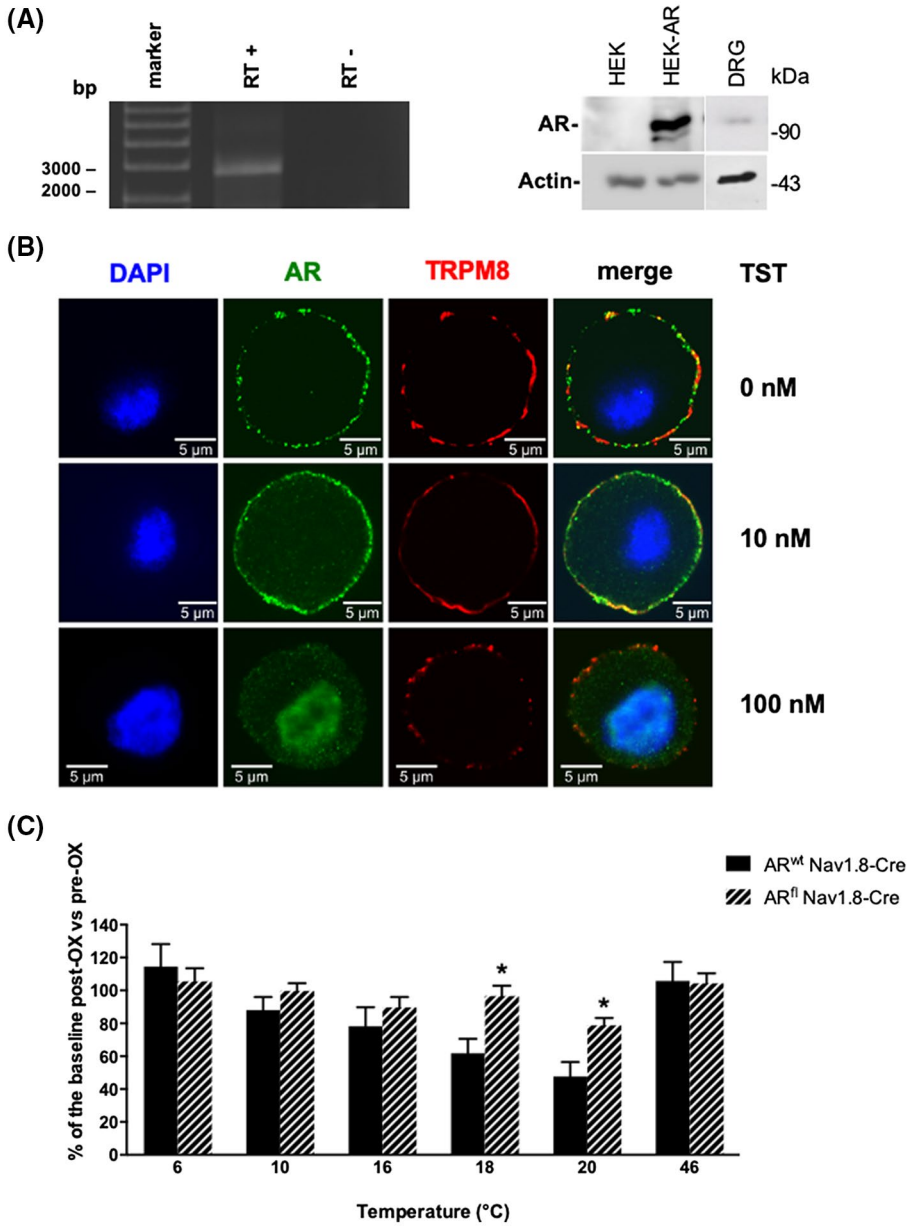

FIGURE 3 Androgen Receptor is expressed in native DRG neurons, where it colocalized with TRPM8 and is involved in TRPM8-mediated cold sensitivity. A, Reverse-transcription PCR showing the specific amplification of full-length AR (2709 bp, left panel) and immunoblot showing AR immunopositive labeling in DRGs at the same molecular weight as in HEK cells overexpressing AR (HEK-AR, right panel). B, Representative confocal images of freshly isolated DRGs treated with 0, 10, and 100 nM of TST, showing colocalization of TRPM8 with AR (green). Note that part of the merged yellow signal is localized at the plasma membrane for the 0 and 10 nM TST treatments. Nuclei are stained with DAPI (blue). C, Comparison of tail withdrawal latencies at specified water bath temperatures in AR^{wt} Nav1.8-Cre and AR^{fl} Nav1.8-Cre mice. Data are expressed as means ± SEM of the ratio of pre- to post-OX thresholds, statistical significance was determined by two-way ANOVA followed by Bonferroni's multiple comparisons test, n = 8-10 (*$P < .05$ compared to AR^{wt} Nav1.8-Cre)

Furthermore, 10 and 100 nM of TST decreased the level of AR in the PM fraction by 63.4% ± 2.5% and 99% respectively, without any significant effect on TRPM8 cell-surface localization (Figure 5B,C). Using fluorescence confocal imaging, we also directly visualized TST binding to AR at the PM of primary cultured DRG neurons from both mice and rats (Figure 5D).

3.6 | TST inhibits TRPM8 through ligand-dependent AR-channel interaction

The association of AR with TRPM8 was first assessed by immunoprecipitation experiments in HEK293 cells transfected with His-tagged TRPM8 with or without CFP-tagged AR. AR was detected in the precipitated complex[30] with TRPM8.

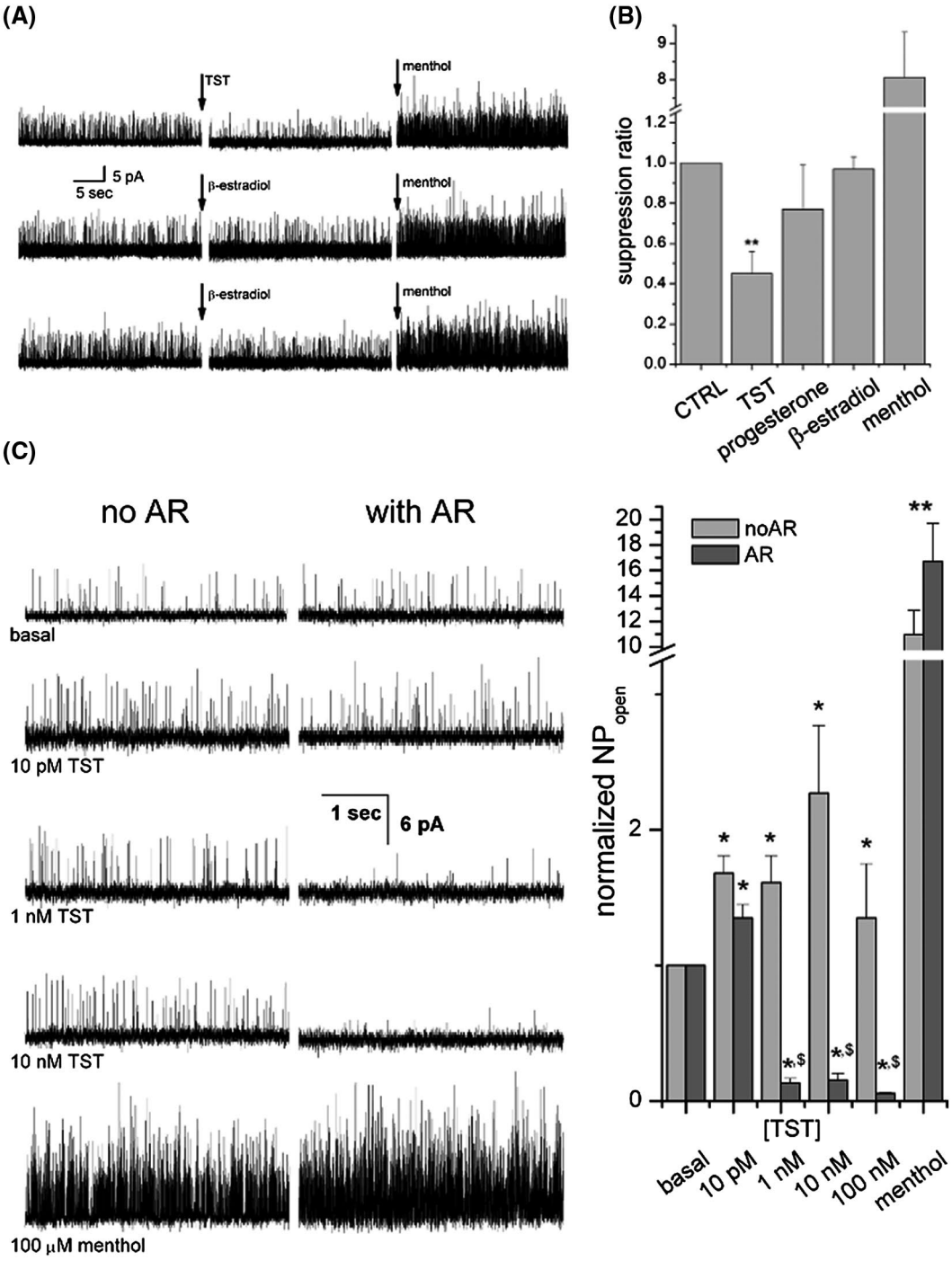

FIGURE 4 TST specifically inhibits TRPM8 through the Androgen Receptor. A, Representative single-channel recordings of TRPM8 activity in cell-attached configuration made at 80 mV in HEK293 cells co-expressing TRPM8 and AR; upper row-basal activity at 20°C (left), and during consecutive applications of testosterone (TST, 10 nM, middle) and menthol (100 μM, right); lower row-same as the upper row, but with β-estradiol (10 nM) instead of testosterone; note the suppression of TRPM8 activity by testosterone but no apparent effect of β-estradiol. B, Quantification of TRPM8 NP_o (normalized to basal levels, mean ± SD) following a 10-minutes treatment with 10 nM testosterone (n = 6), progesterone (n = 7), or β-estradiol (n = 5). C, From top to bottom: representative single-channel recordings of TRPM8 in cell-attached patches from HEK_{M8} (left) and $HEK_{M8/AR}$ (right) cells at 80 mV under basal conditions at 20°C, in the presence of the indicated concentrations of testosterone and following exposure to menthol (100 μM). D, Quantification of TRPM8 NP_o (normalized to basal levels) in the presence of the indicated concentrations of testosterone and 100 μM menthol (n = 7 for HEK_{M8} and 6 for $HEK_{M8/AR}$ cells); note the significant suppression of TRPM8 activity in the presence of AR by testosterone concentrations known to activate the receptor. Data are expressed as means ± SEM, statistical significance was determined by two-way ANOVA followed by Tukey's multiple comparisons test, * and **—significant differences from basal levels at $P < .05$ and $P < .01$, respectively (panels B and D); $—significant difference between HEK_{M8} and $HEK_{M8/AR}$ cells (panel D)

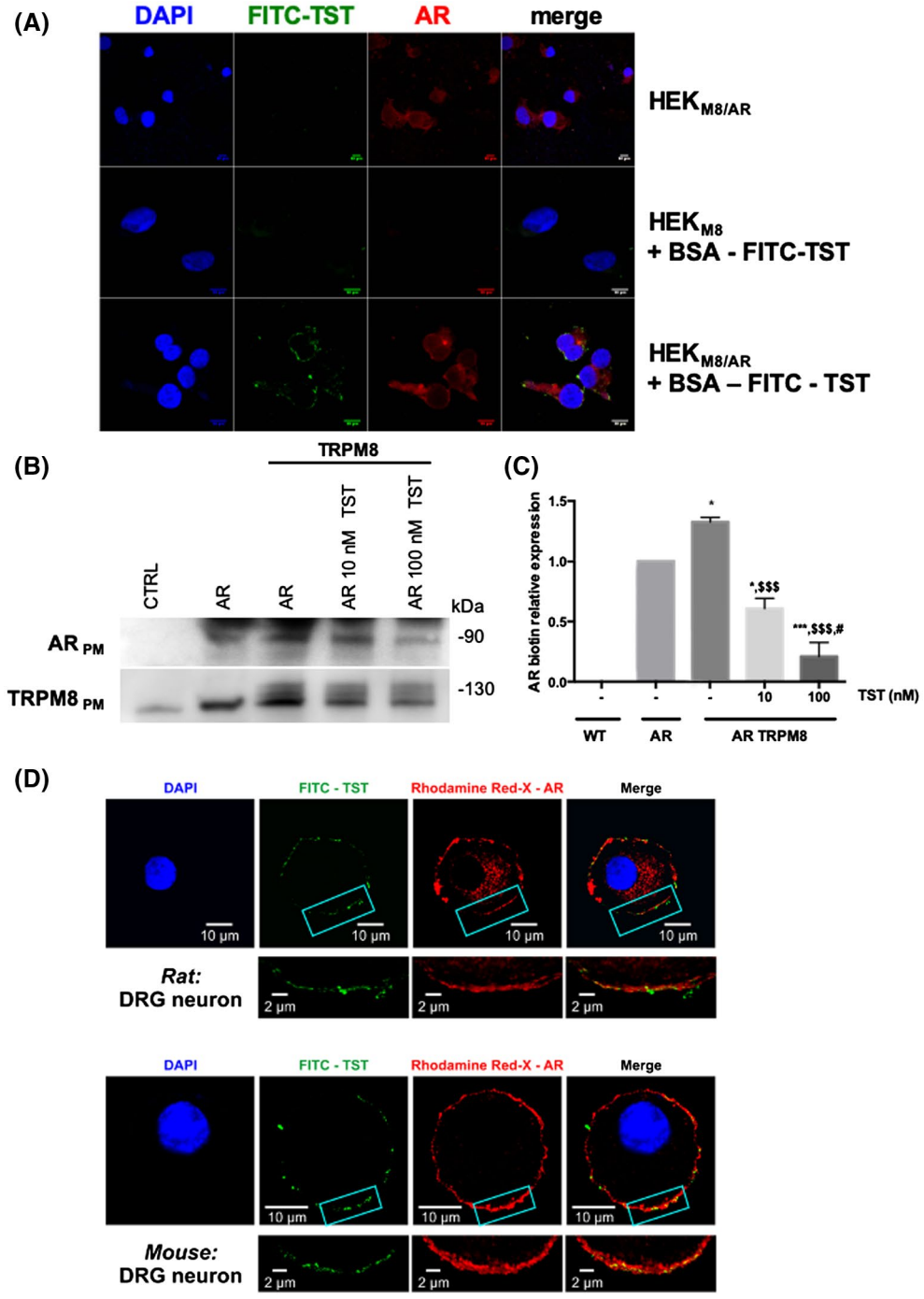

FIGURE 5 TST binds to cell surface Androgen Receptors. A, Representative confocal images of cells stably expressing TRPM8 (HEK_{M8}) transfected with either AR ($HEK_{M8/AR}$) or an empty vector and treated with membrane-impermeable FITC-labeled testosterone (BSA-FITC-TST). AR binding was observed by immunofluorescence depicted in red and nuclei were stained with DAPI, in blue. Cell-surface localization of BSA-FITC-TST (green) is present only in AR-expressing HEK_{M8} cells. B, Cell-surface biotinylation analysis of AR and TRPM8 co-transfected cells treated with 10 or 100 nM of TST. TRPM8 and AR expression were analyzed by immunoblotting the plasma membrane fraction ($TRPM8_{PM}$ and AR_{PM}). C, Bar plots of the relative expression of biotinylated AR and TRPM8. Data are expressed as means ± SEM, statistical significance was determined by two-way ANOVA followed by Tukey's multiple comparisons test, n = 3 independent experiments (*$P < .05$; ***$P < .001$ relative to AR; $^{\$\$\$}P < .001$ relative to AR TRPM8 and $^{\#}P < .05$ relative to AR TRPM8 10nM TST). D, Co-localization of BSA-FITC-TST binding (green) and AR labeled with Rhodamine Red-X (Rhodamine Red-X-AR), visualized in single DRG neurons freshly isolated from rat (top) and mice (bottom), after cell fixation and labeling of the nuclei with DAPI using the multitrack configuration on an LSM 510 META confocal scanner. In each gallery, the upper part shows single confocal x-y images taken from the middle of the entire neuron as indicated. The lower part shows 3-D images obtained by confocal z-sectioning of the boxed region (3 optical slices < 0.6 µm). Note the colocalization of FITC-TST with Rhodamine Red-X-AR

However, no AR band was detected in precipitated complexes from cells that were not transfected with TRPM8 or cells immunoblotted for another protein such as actin, indicating the specificity of the interaction (Figure 6A). Interestingly, the omission of steroids from the culture media resulted in increased AR immunoprecipitation, while a 10min pretreatment of the cells with 10 or 100 nM TST led to the dissociation of the two proteins only for the 100 nM TST condition, what is in line with the results of biotinylation experiments showing the internalization of AR (Figure 6A). To further determine whether TRPM8 interacts directly with the AR, we further performed a GST pull-down assay between GST-tagged TRPM8 N- and C- termini and in vitro translated AR protein. AR protein interacted with both TRPM8 N- and C-terminal peptides but showed 48% ± 7.6% stronger affinity with the N-terminal peptide (Figure 6B).

Finally, we visualized the TRPM8-AR interaction complex at the cellular level using a proximity ligation assay (PLA), which can detect protein-protein binding in situ at single-molecule resolution. PLA for TRPM8-AR produced abundant red puncta in both a HEK293 overexpression system (Figure 6C) and primary DRG neurons (Figure 6D). In addition, in both cell types, treatment with TST resulted in a decrease in the number of puncta by half and altered the localization of the complexes from peripheral to more uniformly distribute in the cytosol.

4 | DISCUSSION

In present study, we have identified the male sex steroid hormone TST as a new endogenous inhibitor of TRPM8-mediated cold sensitivity, acting through the activation of AR at the cell surface (Figure 7).

Our data point to TRPM8 as an environmental cold sensor acutely regulated by steroid sex hormones. Indeed, TST application to sensory neurons not only inhibited the TRPM8 current but also blocked the resulting menthol-evoked AP firing. This electrophysiological evidence explains the higher cold sensitivity of castrated animals at 16-20°C, where TRPM8 is expected to be most active, and the reversal to normal cold sensitivity upon TST reintroduction. It is worth noting that TRPM8 expression in the DRG does not significantly change in castrated mice, suggesting a nongenomic mode of regulation of TRPM8 in these cells, in contrast to that reported for prostate cancer cells.[9,10] The regulation of TRPM8 channel function by androgens may account for age, gender, and individual differences in the perception of cold[31-34] as well as being important for the adaptation of the organism to the ambient temperature depending on plasma levels of TST, which in turn vary depending on seasonal and dietary conditions as well as on physiological and psychosocial state.[35,36] Our data are consistent with the notion that elevated plasma levels of TST, which usually accompany mating behaviors, physical activity, stress, or aggression, would diminish (by inhibiting TRPM8) the impact of environmental cold as a factor that could impede the necessary reaction. The hormonal regulation of TRPM8 activity and hence of cold perception may be of particular significance to males in their adaptation to changes in environmental conditions. In line with this hypothesis, a previous study has shown that in Norwegian men, TST shows bimodal seasonal variations, with peak monthly values in October-November and a nadir in June, and a 19% variation between them.[8] In light of our results, the higher TST levels in the months leading up to winter months could be responsible for TRPM8 inhibition, and therefore, to the reduced sensitivity of men to cold. On the contrary, the regulation of cold sensitivity in females must follow a different mechanism since we did not observe any effect of estrogens or progesterone on TRPM8 activity. It could also be that, in the absence of high TST levels, TRPM8 channels are more active. Nevertheless, recent studies have shown that estrogens and their receptor have a genomic effect on TRPM8 in cancer and dermal tissue.[37-39] The authors of two of these studies have suggested that the lack of estrogens induces TRPM8 overexpression in the skin, and therefore, hypersensitivity to cold in menopausal women.[38,39]

The regulation of ion channels by steroid sex hormones in a nongenomic fashion is quite a widespread phenomenon. It involves various mechanisms and signaling pathways and contributes to gender-related differences in a number of physiological and pathological processes. The molecular mediator of the nongenomic action of TST depends on the cellular and physiological context. Apart from the classic AR, other possible receptors for androgens have been proposed.[14,40-42] Alternatively, TST may bind to the classic AR at the PM. The presence of TRPM8 and AR transcripts co-expression could be supposed based on the recent sequencing data of sensory neurons.[43,44] Our results in vivo and in vitro strongly support the latter hypothesis. Indeed, the inhibition of mild-cold perception by TST is reversed upon genetic ablation of either TRPM8 or AR, demonstrating the recruitment of both proteins. Furthermore, the two proteins are colocalized and interact physically, and the sequence of the AR cloned from DRG samples is the same as that of the canonical receptor. Moreover, using FITC-BSA-TST, we have demonstrated that AR is recruited at the PM of both cultured sensory neurons and a heterologous HEK293 expression system. The presence of AR at the surface of DRGs provides an alternative explanation for recent reports that the TRPM8 channel protein is itself a TST receptor. Indeed, Asuthkar et al have shown that TRPM8 is activated by androgens in the picomolar range.[45] In line with these results, we also observed an increase in TRPM8 activity in response to nanomolar TST concentrations in HEK_{M8} cells. But when TRPM8 was coexpressed with AR ($HEK_{M8/AR}$), the stimulatory effect of TST

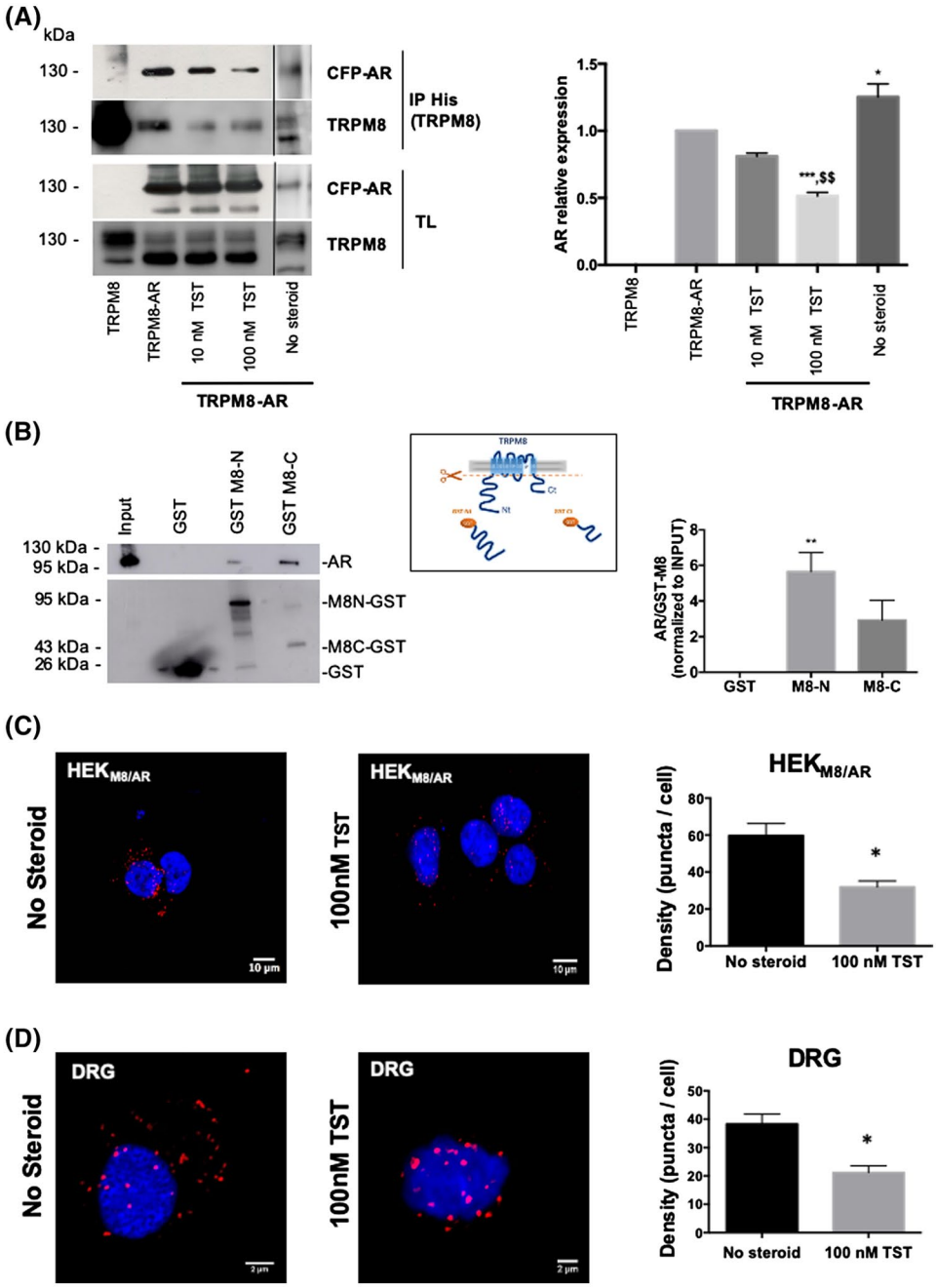

FIGURE 6 The Androgen Receptor interacts directly with TRPM8 in a ligand-dependent way. Immunoblot of co-immunoprecipitation experiments upon treatment with 10 or 100 nM TST, as well as without treatment or with the addition of steroid-free serum. Total lysates (TL) from HEK293 cells transfected with CFP-tagged AR and His-tagged TRPM8 were used for co-immunoprecipitation and subsequent immunoblot analysis. Immunoprecipitation of the channel was confirmed by immunoblotting for TRPM8, and the co-immunoprecipitation with the AR protein was detected using an anti-AR antibody on the immunoprecipitated complex. No co-immunoprecipitation was detected in control immunoblots for AR. Relative AR expression vs actin in the immunoprecipitated fraction is represented in the right panel; data are expressed as means ± SEM, statistical significance was determined by two-way ANOVA followed by Tukey's multiple comparisons test n = 3 independent experiments $*P < .05$ relative to $HEK_{M8/AR}$, $^{\$}P < .05$ relative to $HEK_{M8/AR}$ 10 nM. B, GST pull-down assay of in vitro translated AR and GST or GST fused to the TRPM8 N-terminal tail (GST-Nt) or C-terminal tail (GST-Ct). About 10% of the in vitro translated AR were used for the input of the GST pull-down. Direct interaction of the two proteins is shown in the left panel, which is representative of at least three independent experiments. Quantification of AR/TRPM8 tails interaction normalized over the input is shown in the right panel; $**P < .01$ (student-test). Inset: scheme representing TRPM8 N-terminal tail (GST-Nt) and C-terminal tail (GST-Ct) purification. Proximity Ligation Assay experiments for AR and TRPM8 in HEK293 cells overexpressing AR and TRPM8 ($HEK_{M8/AR}$) C, and native DRG neurons D, upon treatment with 100 nM of TST or vehicle (ethanol). Puncta corresponding to positive PLA results are depicted in red and DAPI-stained nuclei are depicted in blue. The density of puncta is summarized on the right and data are expressed as means ± SEM, statistical significance was determined by Student *t*-test, (n = 4 cells per group, 3 rats); $*P < .05$ relative to untreated $HEK_{M8/AR}$)

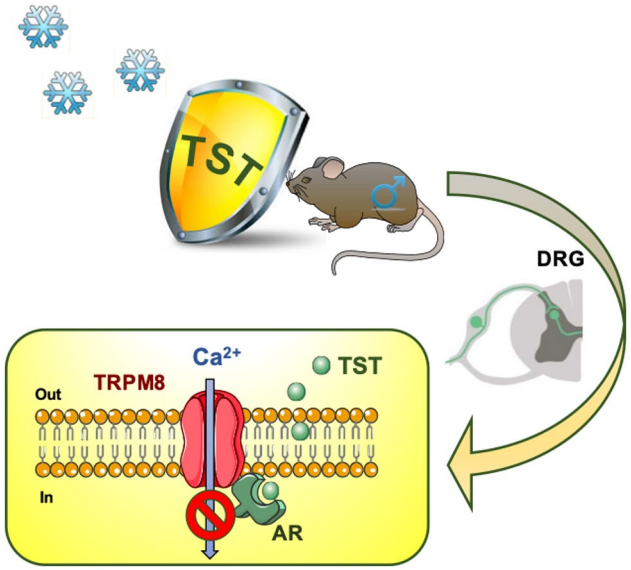

FIGURE 7 TST decreases mild-cold sensitivity in vivo through the inhibition of TRPM8 activity by cell-surface AR. Schematic diagram illustrating that circulating TST inhibits mild-cold perception in male animals through its action on the TRPM8-AR surface complex in sensory neurons (DRG: Dorsal Root Ganglia). Low sensitivity to cold is due to physical interaction of TST-bound AR with the cold receptor TRPM8 with the subsequent inhibition of channel activity

was reversed, leading to a dramatic inhibition of TRPM8 activity at physiological TST concentrations (nanomolar range, Figure 4C,D). We, therefore, propose that in the physiological context and in the presence of endogenous AR, TST acts through its surface receptor and does not exert its effect directly on the channel.

We have previously been shown that the voltage-dependence of the steady-state activation of TRPM8-mediated whole-cell currents in DRG neurons from male rats maintained in the presence of TST demonstrates a roughly 15 mV positive shift compared to DRG neurons from female rats cultured in the presence of 17β-estradiol.[11] Since, according to our data, 17β-estradiol does not affect the TRPM8 channel (see Figure 4B), one could suggest that the inhibitory action of TST via surface AR involves a shift in the voltage-dependence of TRPM8 activation to more positive, nonphysiological membrane potentials. The fact that at the single-channel level, TST decreases the TRPM8 NP_o without affecting single-channel conductance is consistent with this notion. A TST-induced positive shift in the voltage-dependence of TRPM8 activation would result in a higher threshold for a cold or menthol stimulus to induce AP firing in cold-sensitive DRG neurons (Figure 2C), thus, reducing cold sensitivity.

TST, furthermore, modulates TRPM8 activity through AR in a dose-dependent manner, as shown by our electrophysiological measurements as well as biotinylation and interaction assays. At 10 nM, a TRPM8-AR complex is observable at the cell surface, in association with TRPM8 inhibition. Increasing TST concentration to 100 nM causes the detachment of AR from TRPM8 and the expected internalization and nuclear translocation of AR, allowing it to trigger the genomic effects of androgens. The cellular localization of AR is of primary importance for its distinct actions. Nongenomic signals mediated by AR at the membrane have been proposed to be favored in cholesterol-rich lipid-rafts.[46] Interestingly, both AR and TRPM8 have been reported to be localized in lipid rafts.[46,47] TRPM8 responses to cold are enhanced when the channel is located outside lipid rafts, while they are inhibited when it is confined to these domains.[48] Knowing that androgens facilitate the concentration of AR in lipid rafts,[46] it is likely that TST triggers the aggregation of TRPM8-AR complexes in the rafts, resulting in TRPM8 inhibition.

To date, the steroid-hormone-mediated regulation of TRP channels via nongenomic mechanisms has also been demonstrated for seven other members of the TRP family in several physiological contexts: TRPC3, TRPC5, TRPC6, TRPV1, TRPV5, TRPM6, and TRPM3. TRPM6 and TRPV5, which function as gatekeepers of transepithelial Mg^{2+} and Ca^{2+} transport in the kidney, are regulated by estrogens in a nongenomic manner.[49,50] TRPM3 acts as an ionotropic steroid receptor gated by the neuroactive steroid pregnenolone sulfate, which rapidly activates the channel in a heterologous expression system as well as in the native insulin-producing β-cells.[30] Recent studies have shown that the presence of progesterone and, to a lesser extent, progesterone metabolites or 17-estradiol inhibits the channel's response to pregnenolone sulfate within 2-5 minutes, whereas dihydrotestosterone has an inhibitory effect at high concentrations (>1 μM). Interestingly, overlay assays indicate that pregnenolone sulfate, progesterone, and dihydrotestosterone could bind to either TRPM3 or its partner protein.[51] Pregnenolone sulfate has also been shown to inhibit TRPV1,[52] while progesterone reduces TRPC3, TRPC4, TRPC5, and TRPC6 activity.[53,54] The physiological significance of these effects has yet to be revealed, except for TRPM3 inhibition by pregnenolone sulfate, which has been linked to the release of insulin by pancreatic islets.

In conclusion, we have identified TST as a fine regulator of thermosensitivity, making males less sensitive to mild cold. Physiological concentrations of TST act on cell surface AR, which in turn inhibits the mild-cold sensor TRPM8 through direct protein-protein interactions. Interestingly both cytosolic C-terminal and N-terminal domains of TRPM8 both interact with the AR. This pattern of interaction is favored by tetrameric structure of functional TRPM8, where the C- and N-terminal domains of TRPM8 are in close proximity.[55,56] The crystal structure of the NTD has not been determined yet, however, some reports speculated that NTD domain of the AR does not have stable secondary structure in the absence of an interaction with the C-terminal domain

of the AR or another protein.[57,58] It remains to be clarified how these steroid-protein complexes are organized into microdomains and whether they are recruited in other tissues and signaling cascades known to involve these proteins, such as central thermoregulation, prostate and testis function, or cancer pathophysiology.

ACKNOWLEDGMENTS

We thank D. Julius for critical reading and helpful suggestions and for kindly giving us the TRPM8 knockout mice. We thank J. Wood for giving us the Nav1.8-Cre mice created in his lab. We are grateful to F. Van Coppenolle for his help with the testosterone implants. We thank P. Giacobini for critical reading and helpful suggestions. Finally, we thank J. Brocard, L. Pelinski, C. Biot for critical discussion on testosterone chemistry. This work was supported by grants from INSERM, the Ministère de l'éducation nationale and the Région Nord/Pas-de-Calais and INTAS 05-1000008-8223. D. Gkika was supported by a long-term fellowship from the European Molecular Biology Organization (ALTF-161-2006) and by the Institut Universitaire de France (IUF). The authors would like to thank S. Rasika for the English language review.

AUTHOR CONTRIBUTIONS

D. Gkika, J. Busserolles, A. Eschalier, Y. Shuba, R. Skryma, and N. Prevarskaya conceptualized research, D. Gkika, S. Lolignier, A. Bavencoffe, G. Shapovalov, and J. Busserolles designed research; D. Gkika, S. Lolignier, G. P. Grolez, A. Bavencoffe, G. Shapovalov, J. Busserolles, D. Gordienko, A. Kondratskyi, M. Meleine, L. Prival, E. Chapuy, and M. Etienne performed research; D. Gkika, S. Lolignier, G. P. Grolez, A. Bavencoffe, G. Shapovalov, J. Busserolles, D. Gordienko, and A. Kondratskyi analyzed data; D. Gkika, S. Lolignier, and J. Busserolles wrote the paper. D. Gkika, S. Lolignier, A. Bavencoffe, J. Busserolles, D. Gordienko, Y. Shuba, and N. Prevarskaya reviewed and edited the paper.

REFERENCES

1. Vriens J, Nilius B, Voets T. Peripheral thermosensation in mammals. *Nat Rev Neurosci*. 2014;15:573-589.
2. Hensel H. Thermoreception and temperature regulation. *Monogr Physiol Soc*. 1981;38:1-321.
3. McKemy DD, Neuhausser WM, Julius D. Identification of a cold receptor reveals a general role for TRP channels in thermosensation. *Nature*. 2002;416:52-58.
4. Bautista DM, Siemens J, Glazer JM, et al. The menthol receptor TRPM8 is the principal detector of environmental cold. *Nature*. 2007;448:204-208.
5. Colburn RW, Lubin ML, Stone DJ, et al. Attenuated cold sensitivity in TRPM8 null mice. *Neuron*. 2007;54:379-386.
6. Dhaka A, Murray AN, Mathur J, Earley TJ, Petrus MJ, Patapoutian A. TRPM8 is required for cold sensation in mice. *Neuron*. 2007;54:371-378.
7. Götmar A, Hammar M, Fredrikson M, et al. Symptoms in peri- and postmenopausal women in relation to testosterone concentrations: data from the Women's Health in the Lund Area (WHILA) study. *Climacteric*. 2008;11:10.
8. Svartberg J, Jorde R, Sundsfjord J, Bonaa KH, Barrett-Connor E. Seasonal variation of testosterone and waist to hip ratio in men: the Tromso study. *J Clin Endocrinol Metabol*. 2003;88:3099-3104.
9. Zhang L, Barritt GJ. Evidence that TRPM8 is an androgen-dependent Ca^{2+} channel required for the survival of prostate cancer cells. *Cancer Res*. 2004;64:8365-8373.
10. Bidaux G, Roudbaraki M, Merle C, et al. Evidence for specific TRPM8 expression in human prostate secretory epithelial cells: functional androgen receptor requirement. *Endocr Relat Cancer*. 2005;12:367-382.
11. Kondrats'kyi AP, Kondrats'ka KO, Skryma R, Prevars'ka N, Shuba Ia M. Gender differences in cold sensitivity: role of hormonal regulation of TRPM8 channel. *Fiziol Zh*. 2009;55:91-99.
12. Asuthkar S, Elustondo PA, Demirkhanyan L, et al. The TRPM8 protein is a testosterone receptor: I. Biochemical evidence for direct TRPM8-testosterone interactions. *J Biol Chem*. 2015;290:2659-2669.
13. Asuthkar S, Velpula KK, Elustondo PA, Demirkhanyan L, Zakharian E. TRPM8 channel as a novel molecular target in androgen-regulated prostate cancer cells. *Oncotarget*. 2015;6:17221-17236.
14. Thomas P. Membrane androgen receptors unrelated to nuclear steroid receptors. *Endocrinology*. 2019;160:772-781.
15. De Gendt K, Swinnen JV, Saunders PT, et al. A Sertoli cell-selective knockout of the androgen receptor causes spermatogenic arrest in meiosis. *Proc Natl Acad Sci USA*. 2004;101:1327-1332.
16. Stirling CM, Charleston B, Takamatsu H, et al. Characterization of the porcine neonatal Fc receptor–potential use for trans-epithelial protein delivery. *Immunology*. 2005;114:542-553.
17. Zimmermann M. Ethical guidelines for investigations of experimental pain in conscious animals. *Pain*. 1983;16:109-110.
18. Noel J, Zimmermann K, Busserolles J, et al. The mechano-activated K+ channels TRAAK and TREK-1 control both warm and cold perception. *Embo J*. 2009;28:1308-1318.
19. Janssen PA, Niemegeers CJ, Dony JG. The inhibitory effect of fentanyl and other morphine-like analgesics on the warm water induced tail withdrawl reflex in rats. *Arzneimittelforschung*. 1963;13:502-507.
20. Van Coppenolle F, Slomianny C, Carpentier F, et al. Effects of hyperprolactinemia on rat prostate growth: evidence of androgeno-dependence. *Am J Physiol Endocrinol Metab*. 2001;280:E120-E129.
21. Pinchenko VO, Kostyuk PG, Kostyuk EP. Influence of external pH on two types of low-voltageactivated calcium currents in primary sensory neurons of rats. *Biochim Biophys Acta*. 2005;1724:1–7. doi:10.1016/j.bbagen.2005.04.008.
22. Thebault S, Lemonnier L, Bidaux G, et al. Novel role of cold/menthol-sensitive transient receptor potential melastatine family member 8 (TRPM8) in the activation of store-operated channels in LNCaP human prostate cancer epithelial cells. *J Biol Chem*. 2005;280:39423-39435.
23. Livak KJ, Schmittgen TD. Analysis of relative gene expression data using real-time quantitative PCR and the 2(-Delta Delta C(T)) Method. *Methods*. 2001;25:402-408.
24. Gkika D, Flourakis M, Lemonnier L, Prevarskaya N. PSA reduces prostate cancer cell motility by stimulating TRPM8 activity and plasma membrane expression. *Oncogene*. 2010;29:4611-4616.

25. Karashima Y, Talavera K, Everaerts W, et al. TRPA1 acts as a cold sensor in vitro and in vivo. *Proc Natl Acad Sci USA*. 2009;106:1273-1278.
26. Bourinet E, Alloui A, Monteil A, et al. Silencing of the Cav3.2 T-type calcium channel gene in sensory neurons demonstrates its major role in nociception. *Embo J*. 2005;24:315-324.
27. Fernandez JA, Skryma R, Bidaux G, et al. Voltage- and cold-dependent gating of single TRPM8 ion channels. *J Gen Physiol*. 2011;137:173-195.
28. Keast JR, Gleeson RJ. Androgen receptor immunoreactivity is present in primary sensory neurons of male rats. *NeuroReport*. 1998;9:4137-4140.
29. Asuthkar S, Demirkhanyan L, Sun X, et al. The TRPM8 protein is a testosterone receptor: II. Functional evidence for an ionotropic effect of testosterone on TRPM8. *J Biol Chem*. 2015;290:2670-2688.
30. Wagner TF, Loch S, Lambert S, et al. Transient receptor potential M3 channels are ionotropic steroid receptors in pancreatic beta cells. *Nat Cell Biol*. 2008;10:1421-1430.
31. Doeland HJ, Nauta JJ, van Zandbergen JB, et al. The relationship of cold and warmth cutaneous sensation to age and gender. *Muscle Nerve*. 1989;12:712-715.
32. Harju EL. Cold and warmth perception mapped for age, gender, and body area. *Somatosens Mot Res*. 2002;19:61-75.
33. Potkanowicz ES, Caine-Bish N, Otterstetter R, Glickman EL. Age effects on thermal, metabolic, and perceptual responses to acute cold exposure. *Aviat Space Environ Med*. 2003;74:1157-1162.
34. Caudle RM, Caudle SL, Jenkins AC, Ahn AH, Neubert JK. Sex differences in mouse transient receptor potential cation channel, subfamily M, member 8 expressing trigeminal ganglion neurons. *PLoS ONE*. 2017;12:e0176753.
35. Stahl F, Gotz F, Dorner G. Plasma testosterone levels in rats under various conditions. *Exp Clin Endocrinol*. 1984;84:277-284.
36. Gatenbeck L, Eneroth P, Johansson B, Stromberg L. Plasma testosterone concentrations in male rats during short and long-term stress stimulation. *Scand J Urol Nephrol*. 1987;21:139-142.
37. Chodon D, Guilbert A, Dhennin-Duthille I, et al. Estrogen regulation of TRPM8 expression in breast cancer cells. *BMC Cancer*. 2010;10:212.
38. Noguchi W, Ishizuka O, Imamura T, et al. The relationship between alpha1-adrenergic receptors and TRPM8 channels in detrusor overactivity induced by cold stress in ovariectomized rats. *J Urol*. 2013;189:1975-1981.
39. Kubo T, Tsuji S, Amano T, et al. Effects of beta-estradiol on cold-sensitive receptor channel TRPM8 in ovariectomized rats. *Exp Anim*. 2017;66:337-343.
40. Hryb DJ, Khan MS, Rosner W. Testosterone-estradiol-binding globulin binds to human prostatic cell membranes. *Biochem Biophys Res Commun*. 1985;128:432-440.
41. Krupenko SA, Krupenko NI, Danzo BJ. Interaction of sex hormone-binding globulin with plasma membranes from the rat epididymis and other tissues. *J Steroid Biochem Mol Biol*. 1994;51:115-124.
42. Limonta P, Moretti RM, Marelli MM, Motta M. The biology of gonadotropin hormone-releasing hormone: role in the control of tumor growth and progression in humans. *Front Neuroendocrinol*. 2003;24:279-295.
43. Usoskin D, Furlan A, Islam S, et al. Unbiased classification of sensory neuron types by large-scale single-cell RNA sequencing. *Nat Neurosci*. 2015;18:145-153.
44. Li C-L, Li K-C, Wu D, et al. Somatosensory neuron types identified by high-coverage single-cell RNA-sequencing and functional heterogeneity. *Cell Res*. 2016;26:83-102.
45. Asuthkar S, Demirkhanyan L, Sun X, et al. The TRPM8 protein is a testosterone receptor: II. Functional evidence for an ionotropic effect of testosterone on TRPM8. *J Biol Chem*. 2015;290:2670-2688.
46. Freeman MR, Cinar B, Lu ML. Membrane rafts as potential sites of nongenomic hormonal signaling in prostate cancer. *Trends Endocrinol Metab*. 2005;16:273-279.
47. Morenilla-Palao C, Luis E, Fernandez-Pena C, et al. Ion channel profile of TRPM8 cold receptors reveals a role of TASK-3 potassium channels in thermosensation. *Cell Rep*. 2014;8:1571-1582.
48. Morenilla-Palao C, Pertusa M, Meseguer V, Cabedo H, Viana F. Lipid raft segregation modulates TRPM8 channel activity. *J Biol Chem*. 2009;284:9215-9224.
49. Irnaten M, Blanchard-Gutton N, Harvey BJ. Rapid effects of 17beta-estradiol on epithelial TRPV6 $Ca^{(2+)}$ channel in human T84 colonic cells. *Cell Calcium*. 2008;44:441-452.
50. Cao G, van der Wijst J, van der Kemp A, van Zeeland F, Bindels RJ, Hoenderop JG. Regulation of the epithelial Mg2+ channel TRPM6 by estrogen and the associated repressor protein of estrogen receptor activity (REA). *J Biol Chem*. 2009;284:14788-14795.
51. Majeed Y, Tumova S, Green BL, et al. Pregnenolone sulphate-independent inhibition of TRPM3 channels by progesterone. *Cell Calcium*. 2012;51:1-11.
52. Chen SC, Wu FS. Mechanism underlying inhibition of the capsaicin receptor-mediated current by pregnenolone sulfate in rat dorsal root ganglion neurons. *Brain Res*. 2004;1027:196-200.
53. Majeed Y, Amer MS, Agarwal AK, et al. Stereo-selective inhibition of transient receptor potential TRPC5 cation channels by neuroactive steroids. *Br J Pharmacol*. 2011;162:1509-1520.
54. Miehe S, Crause P, Schmidt T, et al. Inhibition of diacylglycerol-sensitive TRPC channels by synthetic and natural steroids. *PLoS ONE*. 2012;7:e35393.
55. Yin Y, Wu M, Zubcevic L, Borschel WF, Lander GC, Lee S-Y. Structure of the cold- and menthol-sensing ion channel TRPM8. *Science (New York, N.Y.)*. 2018;359:237-241.
56. Yin Y, Le SC, Hsu AL, Borgnia MJ, Yang H, Lee S-Y. Structural basis of cooling agent and lipid sensing by the cold-activated TRPM8 channel. *Science*. 2019;363:eaav9334.
57. Bain DL, Heneghan AF, Connaghan-Jones KD, Miura MT. Nuclear receptor structure: implications for function. *Annu Rev Physiol*. 2007;69:201-220.
58. Lavery DN, McEwan IJ. Structure and function of steroid receptor AF1 transactivation domains: induction of active conformations. *Biochem J*. 2005;391:449-464.

SUPPORTING INFORMATION

Additional Supporting Information may be found online in the Supporting Information section.

How to cite this article: Gkika D, Lolignier S, Grolez GP, et al. Testosterone-androgen receptor: The steroid link inhibiting TRPM8-mediated cold sensitivity. *The FASEB Journal*. 2020;34:7483–7499. https://doi.org/10.1096/fj.201902270R